NUMERIČKA ANALIZA UTICAJA OSNOVNIH RADNIH PARAMETARA NA KARAKTERISTIKE EJEKTORSKOG SOLARNOG HLAĐENJA

NUMERICAL ANALYSIS OF THE INFLUENCE OF BASIC OPERATING PARAMETERS ON THE PERFORMANCE CHARACTERISTICS OF SOLAR-DRIVEN EJECTOR COOLING

Branislav PETROVIĆ*, **Milan GOJAK, Đorđe KOZIĆ**
Faculty of Mechanical Engineering, University of Belgrade, Serbia

https://doi.org/10.24094/kghk.020.51.1.129

Razvoj ejektorskih solarnih sistema hlađenja, sve više zaokupira pažnju istraživača, pre sve kao primer korišćenja obnovljivog izvora energije. Apsorpcioni i adsorpcioni rashladni sistemi imaju velike investiocione troškove, dok su sistemi sa ejektorom zbog nepostojanja pokretnih delova, znatno pouzdaniji. Osim toga, ejektorsko hlađenje ima niz prednosti usled niske cene, jednostavne konstrukcije, pouzdanog rada, dugog veka trajanja i gotovo nikakvog održavanja. Jedina slabost ovog sistema je mala efikasnost i netolerancija na odstupanje od radnih uslova. U radu je razvijen matematički model sa algoritmom, koji se oslanja na zakone termodinamike, kao i na zakone održanja mase i impulsa. Na osnovu dobijenog modela, za dva radna fluida R134a i R290, prikazan je uticaj temperature na osnovne parametre sistema i to u opsegu temnperatura radnog fluida u generatoru (80-100 °C), isparicaču (5-15 °C) i kondenzatoru (33-40 °C). Kao glavni pokazatelji se ističu: odnos karakterisitčnih površina A_r (kao geometrijski parametar ejektora), koeficijent usisavanja ejektora, efikasnost ejektora i COP. Pokazuje se da geometrija ejektora, kao i vrsta radnog fluida imaju značajan uticaj na performanse ejektorskog rashladnog sistema.

Ključne reči: *ejektor; rashladni sistem; solarna energija; radni parametri; karakteristike; kompjuterska simulacija*

Researchers are becoming growingly interested in the development of solar-driven ejector cooling systems, primarily due to their potential to be used as renewable energy sources. Absorption and adsorption refrigeration systems not only involve considerable investment but are also much less reliable than the ejector refrigeration systems, which do not contain any movable parts. In adition, ejector refrigeration has the advantage of low capital cost, simple design, reliable operation, long lifespan and almost no maintance. The only weakness of this system is the low efficiency and its intolerance to deviations from design operation condition.The paper develops a mathematical model with an algorithm which is based on the laws of thermodynamics and the principles of mass and momentum conservation. Based on the obtained model, the influence of temperature on the basic system parameters for two working fluids, R134a and R290, is presented. The working fluid temperature ranges are 80-100°C in the generator, 5-15°C in the evaporator and 33-40°C in the condenser. The important performace indicators are the characteristic ejector area ratio Ar (as a geometrical ejector parameter), ejector entrainment ratio, ejector efficiency and the COP. The results indicate that ejector geometry and working fluid type have a major impact on the ejector cooling system's performance.

Key words: *ejector; refrigeration system; solar energy; operating parameter; performance characteristics; computer simulation*

1 Introduction

The sun is a renewable energy source, which can be used for cooling, heating, but also as electricity production. The solar-driven ejector cooling system is one example of such system. In this article, we will examine the systems which are used to air-condition various spaces during daytime – the solar cooling systems. Free solar energy exploited by the solar collector is quantitative and qualitative enough to produce the motive fluid for an ejector refrigeration system. Nevertheless, according to the characteristic of an ejector and the initial investment cost, the solar refrigerator system is suitable for the application of air-conditioning system rather than that of the refrigeration purposes. The applicability of the system is determined by overall COP, which is the essential parameter for these systems. Following formula can be used to determine the overall performance coefficient of the solar refrigeration cycle [13]:

$$\mathrm{COP}_{\mathrm{overall}} = \eta_{\mathrm{coll}}\eta_G \mathrm{COP} \tag{1}$$

The efficiency of a solar system is determined by following factors: the collector type, solar radiation intensity, and the system operating conditions. The COP of the ejector refrigeration system will be specified afterwards.

Collector efficiency can be calculated using equation (2):

$$\eta_{\mathrm{coll}} = Q_{\mathrm{ul}} / A_{\mathrm{coll}} I \tag{2}$$

---

* Corresponding author's e-mail: bpetrovic@mas.bg.ac.rs

where Q_{in} is the heat trasferretd with water from the collectors to the generator, A_{coll} is the total collection area, and I is solar radiation.

On the other hand, the generator efficiency formula is:

$$\eta_G = Q_\mathrm{G} / Q_\mathrm{ul} \tag{3}$$

where Q_G is the heat transfered to working fluid.

It is evident that the performance of the refrigeration system itself is not the only parameter that affects the overall performance of the solar refrigerator, but the thermal efficiency of solar collector as well. In agreement with the above relation, the mathematical model used to predict the overall system performance is therefore always presented in two parts, the prediction of ejector refrigerator and solar collector performance, respectively. In this work, we are solely focused on the prediction of ejector performances.

Nomenclature

A	cross-section area (m^2)	*p*	pressure (MPa)	*Greek symbols*		G	generator
Ar	ejector area ratio	*p′*	mixing pressure (kPa)	μ	entrainment ratio	ul	inlet
COP	coefficient of performance	*Q*	heat load (kJ)	*η*	efficiency	meš	mixing
h	specific enthalpy (kJ kg^{-1})	*s*	entropy (kJ kg^{-1}1 K^{-1})	Π	pressure lift ratio	m	nozzle
ϰ	heat capacity ratio	*T*	temperature (°C)	*Subscripts*		outlet	iz
ṁ	mass flow rate (kg s^{-1})	*V*	velocity (m s^{-1})	K	condenser	0-5	ejector locations
M	Mach number	*W*	work (kJ)	D	diffuser	coll	collector
*M**	critical Mach number			I	evaporator	ej	ejector

2 Ejector Cooling System Analysis

In addition to an ejector and three heat exchangers, namely the steam generator (G), condenser (K) and evaporator (I), the ejector cooling system consists of a pump and a expansion valve (Figure 1) [11].

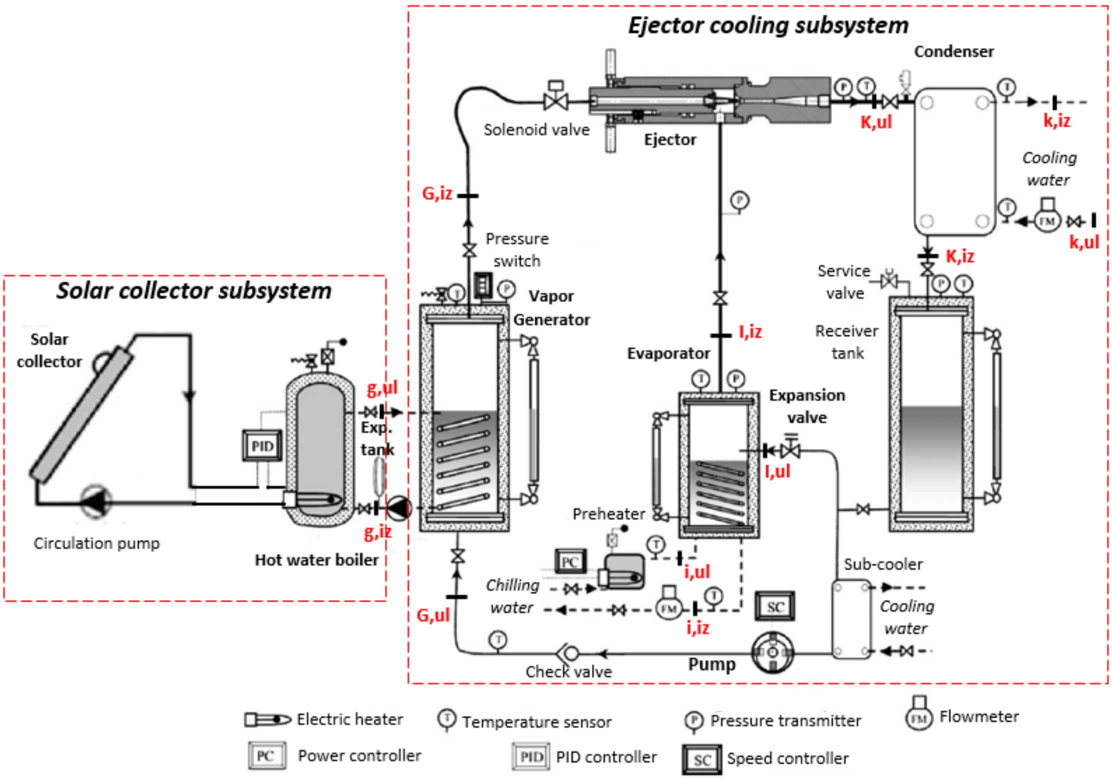

Figure 1. Schematic diagram of solar-assisted ejector cooling system.

The liquid primary fluid of high pressure and temperature and negligible speed, evaporates due to heat flux $\dot{Q}_\mathrm{G}$ supplied from the heat source. The generated vapour then enters the ejector and expands to supersonic speed and reduced pressure in the convergent-divergent nozzle (primary nozzle). The reduced pressure after the nozzle enables the low-pressure vapour (secondary fluid) from the evaporator to flow to the ejector suction chamber. The two streames are mixed, generating a shock wave and a significant rise in pressure in the part of the ejector with constant area. A normal shock wave is generated only in the case of one-dimensional ejector analysis. However, in actual circumstances, because of a thick boudary layer, the shock wave is not fully normal, due to the occurrence of complex oblique shock patterns. This mixed flow becomes subsonic and is further slowed down in the ejector diffuser. At the diffuser outlet, the two mixed flow reach the adequate increased pressure in the condenser. The mixed primary and secondary fluids are turned into liquid state in the condenser, while the $\dot{Q}_K$ heat flux is rejected to the heat sink. The liquid working fluid is then divided into two separate circuits. The larger part of the resulting liquid refrigerant returns to the generator, raising the pressure in the supply pump, while the remaining refrigerant enters the evaporator via the expansion valve. Cooling effect $\dot{Q}_I$ is then generated in the evaporator, and the full cycle is over. All basic processes are illustrated in the form of *T-s* and *h-s* diagram (Figure 2) [1],[2].

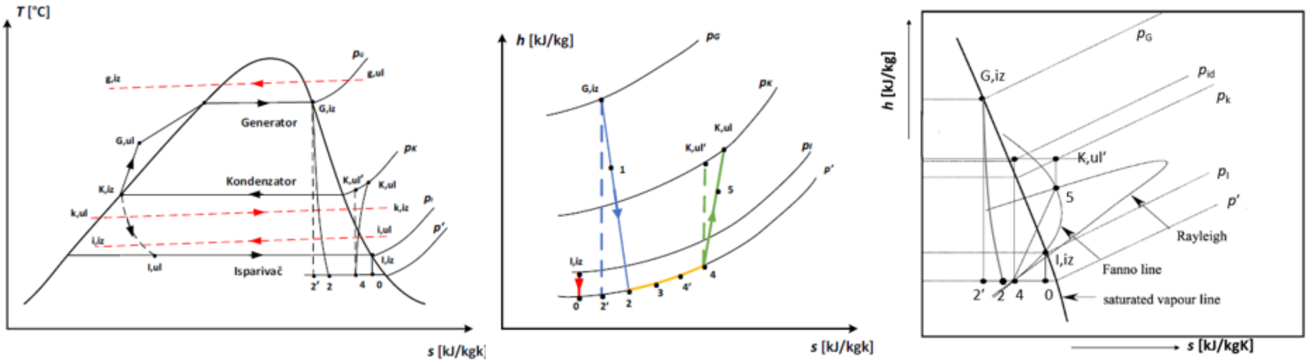

Figure 2. a) Thermodynamic cycle of the ejector refrigeration system for R134a; b) h-s diagram of ejector working processes; c) Mollier's chart of an ejector.

3 Ejector analysis

It is shown that the ejector is one of the primary and most important parts of an ejector cooling system, as it takes on the role of a compressor, which is necessary in convencional cooling systems. At the same time, ejector is the most problematic element, in which turbulent mixing of two fluid flows, supersonic flow with a shock wave and other phenomena occur. Figure 2 is the schematic diagram of an ejector consisting of a primary nozzle, a mixing chamber, an ejector part with constant area (throat) and a diffuser [12]. The figure also shows primary and secondary fluids' pressure and speed changes occurring in the ejector.

An ideal ejector would achieve a mixing pressure p_{id} at the ejector outlet during an isentropic process, where the shock wave would not be considered (Figure 2.c). The processes inside the ejector are largely irreversible due to the turbulent mixing of the primary and secondary fluids, even if the loss due to the shock is eliminated.

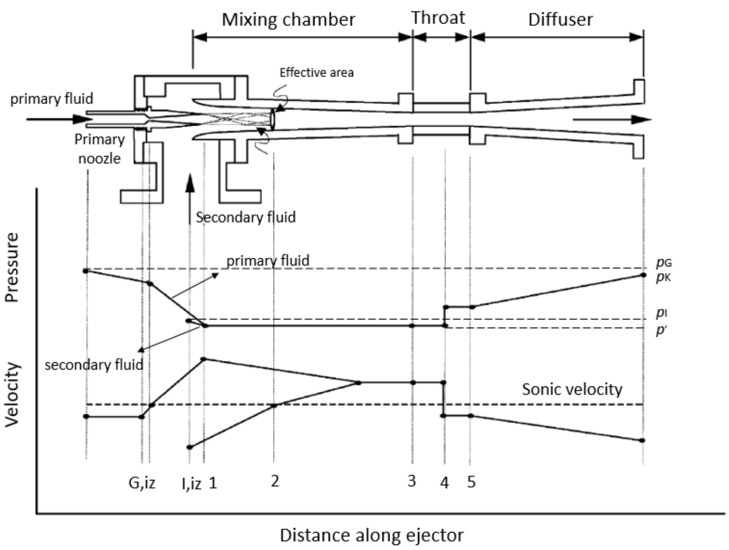

Figure 3. Schematic view and the variation in stream pressure and velocity as a function of location along ejector.

The following assumptions need to be introduced in order to perform an analysis of the processes inside the ejector:

1. Fluid flow through the ejector is one-dimensional, stationary and adiabatic;
2. The velocities of the primary fluid, secondary fluid and outlet mixture at ejector inlet and outlet are negligible;

3. The primary and secondary fluid mixing process takes place under constant pressure , lower than the pressure in the evaporator, in the part of the evaporator with constant area;
4. All flow losses in real adiabatic expansion and compression processes compared to isentropic processes are considered using the nozzle (η_{m}), diffusor (η_{d}) and mixing chamber efficiencies ($\eta_{\mathrm{meš}}$).
5. The primary and secondary fluids are considered as ideal gas, with constant c_p and $\varkappa$ values [15];
6. Normal shock occurs at the end of constant-area mixing chamber.

The theory of one-dimensional ejector analysis was first introduced by Keenan at al. It has been used as the theoretical base in ejector design for the past fifty years. The theory is based with the principles of the mass and momentum conservation as well as on the law of thermodynamics for the control volume, where the working fluid is based on an ideal gas dynamics.

4 Energy Analysis

The energy analysis of the ejector cooling system begins with the equation (4), based on the first law of thermodynamics for control volume:

$$\dot{Q}_{AB} + \dot{W}_{\mathrm{teh},AB} = \dot{m}\left[h_B - h_A + \frac{\vec{V}_B^2 - \vec{V}_A^2}{2} + g(z_B - z_A) \right] \tag{4}$$

While passing through the primary nozzle, the primary fluid from the generator reaches the speed of sound (M=1) in the nozzle throat. The increase in cross section area in the divergent part of the primary nozzle then results in a pressure drop and acceleration to supersonic speed (M>1). Based on equation (4), the speed of the primary fluid at the inlet to the mixing chamber is calculated. The same method is used to calculate the speed of the secondary fluid from the evaporator to the same mixing chamber cross-section (friction losses are not considered).

$$\vec{V}_2 = \sqrt{2\eta_m (h_{\mathrm{G,iz}} - h_2')} \quad \vec{V}_0 = \sqrt{2(h_{\mathrm{I,iz}} - h_0)} \tag{5}$$

The primary and secondary fluids are mixed in the mixing chamber, and the mass conservation equation is used to calculate the mass flow rate of the mixed fluid as follows:

$$\dot{m}_m = \dot{m}_{\mathrm{G}} + \dot{m}_{\mathrm{I}} = \dot{m}_{\mathrm{G}}(1+\mu) \tag{6}$$

where μ is the ejector entrainment ratio, represented by the fluids' mass flow rate ratio towards the evaporator and generator respectively.

The mixed fluid speed mathematical expression is obtained on the basis of the momentum conservation equation (7), considering the $\eta_{\mathrm{meš}}$ mixing chamber efficiency, defined by the $\vec{V}_4^2 / \vec{V}_{4'}^2$ ratio [3].

$$\dot{m}_{\mathrm{G}}\vec{V}_2 + \dot{m}_{\mathrm{I}}\vec{V}_0 = \dot{m}_m\vec{V}_4 \qquad \rightarrow \qquad \vec{V}_4 = \frac{\vec{V}_2 + \mu'\vec{V}_0}{1+\mu'}\sqrt{\eta_M} \tag{7}$$

The μ' ejector entrainment ratio is assumed, since this value is unknown in the initial calculation stage. The mixed flow enthalpy is calculated on the basis of the energy balance equation:

$$\dot{m}_{\mathrm{G}}(h_2 + \frac{\vec{V}_2^2}{2}) + \dot{m}_{\mathrm{I}}(h_0 + \frac{\vec{V}_0^2}{2}) = \dot{m}_m(h_4 + \frac{\vec{V}_4^2}{2}) \qquad \rightarrow \qquad h_4 = \frac{h_{\mathrm{G,iz}} + \mu' h_{\mathrm{I,ul}}}{1+\mu'} - \frac{\vec{V}_4^2}{2} \tag{8}$$

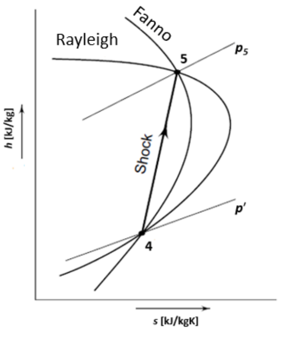

It is assumed that a normal shock wave occurs at the end of constant-area mixing chamber. In this narrow zone, the speed suddenly drops and the pressure surges. As a result, the mixture pressure at ejector outlet is higher than the secondary fluid's initial pressure. Based on the mass conservation, momentum conservation and energy balance equations, the following values are obtained:

$$\dot{m}_{\mathrm{G}} + \dot{m}_I = \rho_4 V_4 A_{\mathrm{meš}} = \rho_5 V_5 A_{\mathrm{meš}} \tag{9}$$

$$(p_5 - p_4)A_{\mathrm{meš}} = (\vec{V}_5 - \vec{V}_4)(\dot{m}_G + \dot{m}_I) \tag{10}$$

$$h_4 + \frac{\vec{V}_4^2}{2} = h_5 + \frac{\vec{V}_5^2}{2} \tag{11}$$

Figure 4. Process in shock diffuser.

Condition 5 following the shock wave is obtained at the point of intersection of two curves giving the solution of these three equations, with the use of the equation of state where steam property tables may be used. The solutions of the equations (9) and (10) are illustrated with a Fano line, while the solutions of the equations (9) and (10) are illustrated with a Rayleigh line [15]. Subsonic fluid speed is achieved after the shock wave. Based on the assumption that the speed of the primary and secondary fluid mixture at diffusor outlet is negligible, and considering the diffusor efficiency, the following is established:

$$h_{\mathrm{K,ul}} - h_4 = \frac{\vec{V}_4}{2} = \frac{h_{\mathrm{K,ul}}{}' - h_4}{\eta_d} \tag{12}$$

The final expression for calculating ejector entrainment coefficient [2] is expressed with equation (13) on the basis of equations (7) and (12):

$$\mu = \frac{\sqrt{2\eta_m (h_{\mathrm{G,iz}} - h_{2'})} - \sqrt{2(h_{\mathrm{K,ul'}} - h_4)/(\eta_d \eta_{me\check{s}})}}{\sqrt{2(h_{\mathrm{K,ul'}} - h_4)/(\eta_d \eta_{me\check{s}})} - \sqrt{2(h_{\mathrm{I,ul}} - h_0)}} \tag{13}$$

5 Performance characteristics

The performance characteristics of the ejector and the ejector cooling system are determined on the basis of the following parameters: entrainment ratio (μ), coefficient of performance (COP), pressure lift ratio (Π), ejector efficiency (η_{ej}) and ejector area ratio (A_r).

The most important parameters used to describe the performance of ejectors in cooling systems are ejector entrainment ratio and pressure lift ratio [8].

$$\mu = \frac{\dot{m}_I}{\dot{m}_G} \quad \Pi = \frac{p_{\mathrm{K}}}{p_I} \tag{14}$$

Ejector entrainment ratio is one of the crucial ejector system parameters, and the basic calculation of the ejector cooling system relies on as accurate calculation of this value as possible. It is defined by the ratio of the mass flow rate of the secondary fluid from the evaporator and the mass flow rate of the primary fluid from the generator. Ejector entrainment ratio is related to the energy efficiency of the cooling cycle, whereas pressure lift ratio is a measure of the cycle's working range. Pressure lift ratio limits the temperature at which $\dot{Q}_{\mathrm{K}}$ heat flux is rejected from the cooling water to the heat sink during condensation. Therefore, the best ejector will have the highest values of ejector entrainment ratio and pressure lift ratio under the given operating conditions.

The main energy indicator of ejector cooling system cycle quality is expressed using the ratio between the useful cooling capacity to the gross energy input into the cycle required to achieve the cooling capacity.

$$\mathrm{COP} = \frac{\dot{Q}_{\mathrm{I}}}{\dot{Q}_{\mathrm{G}} + \dot{W}_{\mathrm{P}}} \approx \mu \frac{h_{\mathrm{I,iz}} - h_{\mathrm{I,ul}}}{h_{\mathrm{G,iz}} - h_{\mathrm{K,iz}}} \tag{15}$$

where $\dot{Q}_{\mathrm{I}} = \dot{m}_{\mathrm{I}}(h_{\mathrm{I,iz}} - h_{\mathrm{I,ul}})$ is evaporator capacity, $\dot{Q}_{\mathrm{G}} = \dot{m}_{\mathrm{G}}(h_{\mathrm{G,iz}} - h_{\mathrm{G,ul}})$ is generator capacity, and $\dot{W}_{\mathrm{P}}$ is pump power, which is not considered in this paper.

Ejector efficiency is determined on the basis of the following equation [8]:

$$\eta_{\mathrm{ej}} = \left(\frac{\dot{m}_G + \dot{m}_I}{\dot{m}_G}\right)\left(\frac{h_{\mathrm{K,ul}} - h_{\mathrm{I,iz}}}{h_{\mathrm{G,iz}} - h_{2'}}\right) = (1+\mu)\frac{h_{\mathrm{K,ul}} - h_{\mathrm{I,iz}}}{h_{\mathrm{G,iz}} - h_{\mathrm{I,iz}}} \tag{16}$$

One of the main geometrical parameters important for ejector design is the ratio of the mixing chamber's (A_3) and nozzle throat's (A_1) cross-section areas, calculated as follows [14]:

$$A_r = \frac{A_3}{A_1} = \left(\frac{V_1\rho_1}{\dot{m}_{\mathrm{G}}}\right)\left(\frac{\dot{m}_{\mathrm{G}} + \dot{m}_{\mathrm{I}}}{V_4\rho_4}\right) = \frac{p_{\mathrm{G}}(1+\mu)^{1/2}(1+\mu T_{\mathrm{I}}/T_{\mathrm{G}})^{1/2}(2/(\kappa+1))^{1/(\kappa-1)}(1-2/(\kappa+1))^{1/2}}{p_{\mathrm{K}}(p_5/p_{\mathrm{K}})^{1/\kappa}(1-(p_5/p_{\mathrm{K}})^{(\kappa-1)/\kappa})^{1/2}} \tag{17}$$

6 Computational Procedures

In addition to the basic equations describing the states of fluids in the ejector, the introduction of more March numbers [1], [4], [5] is required, including their critical values. A numerical calculation analysis has been developed on the basis of the mathematical model in order to foresee the influence of operating parameters on the performance characteristics of the ejector cooling system (μ, COP, η_{ej} and A_r). The main characteristic of this calculation is the need to execute two iterations so as to obtain the real p' and μ values, which are interrelated. These two values are obtained by comparing the assumed with the real μ value and the initially determined p_{K} value with the calculated p_{K}' value [1], based on the aforementioned Mach number values, and with the set error value.

Upon the completion of the numerical program in Matlab, the following operating parameters have been adopted: working fluid temperature in the evaporator (T_{I}): 5 °C, 10 °C and 15 °C; working fluid temperature in the generator (T_{G}) is adopted in the 80-100 °C range, while the operating temperature in the condenser is given for either 33 °C or 40 °C.

Table 1. Numerical procedure for the solution of the model.

Step	*Numerical calculation algorithm*
1	Choose refrigerant; enter T_G, T_I, p_K, Q_I, and κ , η_m, η_d, $\eta_{meš}$ values
2	Find $p_G\,(T_G)$, $p_I\,(T_I)$, $h_{G,iz}=h''(T_G)$, $s_{G,iz}=s''(T_G)$, $h_{I,iz}=h''(T_G)$, $h_{K,iz}=h'(p_K)$ values
3	Assume p' value
4	Calculate $V_2=[2\eta_m(h_{G,iz}-h_2')]^{1/2}$; $h_2'=f\,(p', s_2')$, $s_{G,iz}=s_2'$
5	Calculate $V_0=[2(h_{I,iz}-h_0)]^{1/2}$; $h_0=f\,(p', s_0)$, $s_{I,iz}=s_0$
6	Assume μ' value
7	Calculate V_4 value (using mass conservation equation) Calculate h_4 value (using energy balance) Find $h_{K,ul}$ using $h_{K,ul}=h_4+V_4^2/2$
8	Find $h_{K,ul}'=f\,(p_K, s_4)$; $s_4=f\,(p', h_4)$ in overheated vapour condition
9	Calculate the real value of μ on the basis of the equation (13)
10	Find $\lvert\mu-\mu'\rvert \leq \varepsilon_1$ If the difference is within the range of setpoint error, the program continues to operate. If the difference exceeds setpo-int error, the μ' value is again assumed (Step 6).
11	Calculate Mach number values: $M_{G,2}$; $M_{I,2}$ Calculate Mach number critical values: $M_{G,2}^*$; $M_{I,2}^*$ Calculate M_4^*, M_4, M_5 values Calculate pressure values: p_5, p_K'
12	Find $\lvert p_K-p_K'\rvert \leq \varepsilon_2$ If the difference is within the range of setpoint error, the program continues to operate. If the difference exceeds setpo-int error, the p' value is again assumed (Step 3).
13	Caclculate: $\dot{m}_I=Q_I/(h_{I,iz}-h_{K,iz})$; $\dot{m}_G=\dot{m}_I/\mu$ $Q_K=(\dot{m}_G+\dot{m}_I)((h_{K,ul}-h_{K,iz})$; $Q_G=\dot{m}_G(h_{G,iz}-h_{K,iz})$ Based on the given equations, we finally get COP and A_R values

In addition, the influence on the aforementioned performance characteristics of nozzle efficiency (η_m) in the 0.8-1.0 range is observed, as well as diffuser efficiency η_d=0.8:1

For each of these conditions, a simulation was performed for two working fluids, R134a and R290. The input data for these refrigerants was retrieved from the NIST REPROP database [16]. The perofrmance characteristics of these two fluids are given in Table 2 [10].

Table 2. Working fluids for ejector refrigeration system used in paper

Type of refrigerant	*Boiling pointat at 1 atm (°C)*	*Molecular mass (kg/kmol)*	*Latent heatat 0 °C (kJ/Kg)*	*Global warming potential (GWP)*	*Ozone depletion potential (ODP)*	*Wet/dry vapour*
R134a	-26.1	102.03	190.9	0.26	0.002	Wet
R290	-42.1	44.1	357.2	3	0	Wet

7 Results

The numerical calculation results show the influence of the working fluid temperature in the generator, evaporator and condenser and also the influence of nozzle and diffuser efficiencies on the performance characteristics of the ejector cooling system.

Ejector entrainment ratio (μ), area ratio (A_r), COP and ejector efficiency (η_{ej}) are four important, interdependent ejector cooling system parameters, which vary according to the operating conditions and suitable working fluids.

Based on the presented algorithm, it can be concluded that the ejector entrainment ratio for both working fluids increases with the temperature rise in the generator, when the values of the other operating parameters are maintained constant (Figure 5 and Figure 6). The explanation for the increase in ejector entrainment ratio due to higher temperature T_G is the fact that higher working fluid temperature, i.e. higher pressure in the generator requires a lower mass flow rate of the primary fluid from the generator in order to entraint a fixed amount of mass flow rate from the evaporator ($\mu=\dot{m}_I/\dot{m}_G$). Conversely, if there is a working fluid temperature drop in the generator, the mass flow rate of the primary fluid is equal to that of the secondary fluid, and the secondary fluid is not entrained in the ejector. In addition, the presented diagram shows that when the working fluid temperature in the evaporator rises, for the set T_G and T_K temperatures, the ejector entrainment ratio increases since higher evaporation pressure requires a smaller amount of the primary fluid. For this reason, a lower evaporation temperature requires a higher working fluid temperature in the generator in order to draw the secondary fluid from the evaporator, into the ejector. Ejector entrainment ratio decreases with the increase in the working fluid temperature in the condenser, because of the rate of increase in the primary mass flow from the generator is larger than that of the secondary mass flow from the evaporator.

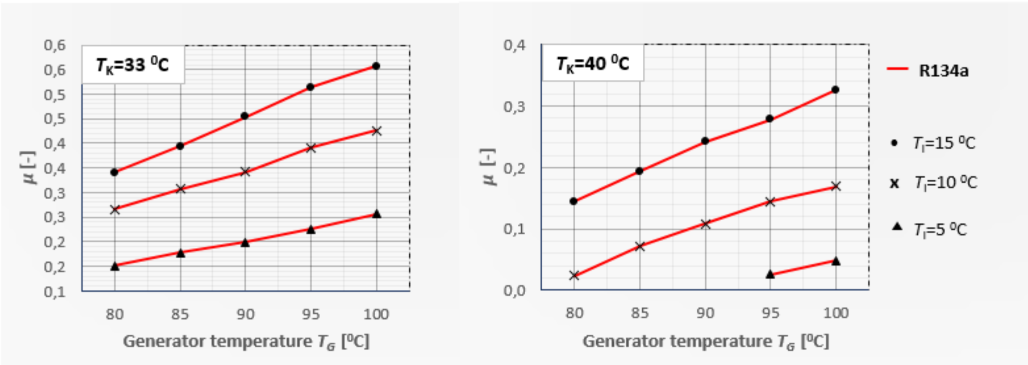

Figure 5. Effect of operating conditions on ejector entrainment ratio for working fluid R134a.

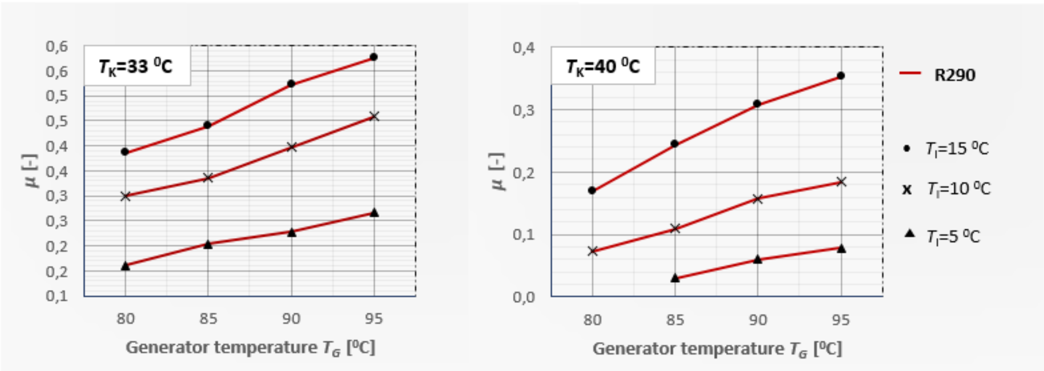

Figure 6. Effect of operating conditions on ejector entrainment ratio for working fluid R290.

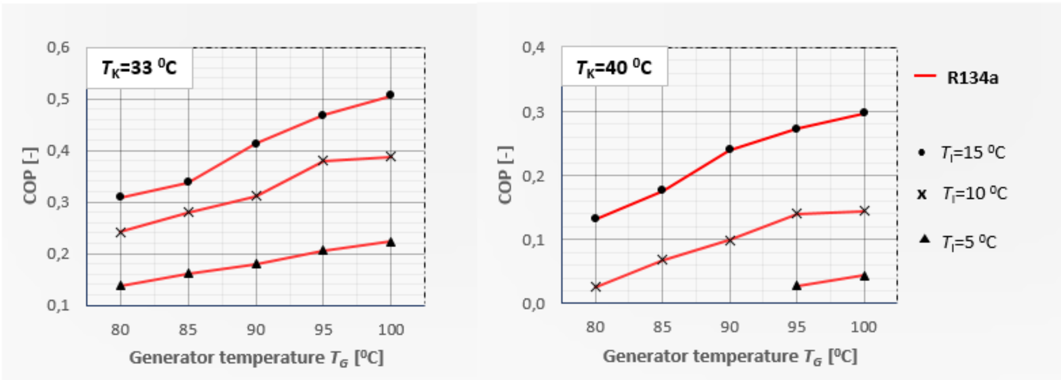

Figure 7. Effect of operating conditions on system COP for working fluid R134a.

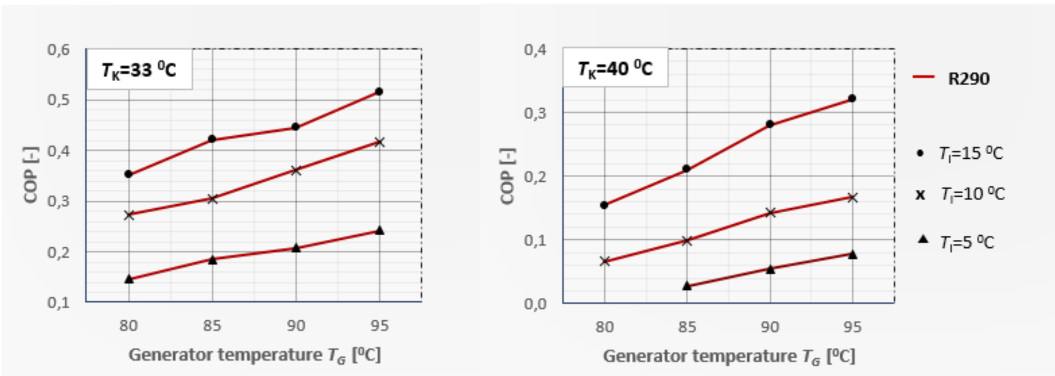

Figure 8. Effect of operating conditions on system COP for working fluid R290.

The diagram illustrating the dependence of the operating parameters on COP value (Figure 7 and Figure 8) is of similar nature as the diagram of the entrainment ratio. Value of COP rises with the increase in the working fluid temperature in the generator. The reason is that the enthalpy change in the generator is small for a fixed cooling capacity, so the COP value (based on equation 15) mostly depends on the ratio of the mass flow rates of the primary and secondary fluids. The diagram also indicates that a higher T_G temperature is required in order to achieve the same COP value at a lower evaporation temperature. However, a higher working fluid temperature in the generator requires a higher value of temperature range from the low-grade heat source. The COP value of the R290 working fluid is higher than that of the R134a refrigerant. Furthermore, the R290 working fluid temperature in the generator is limited to 95 °C due to the critical temperature of this refrigerant, which is 96.7 °C. The environmentally friendly R134a refrigerant has both a low boiling point (-26.5 °C) at atmospheric pressure and a low critical temperature (101.1 °C). A rise in evaporation temperature is followed by a rise in the COP value due to the influence of ejector entrainment ratio on the COP. Due to the rise in condensation temperature, ejector entrainment ratio drops, which causes a decrease in the COP value.

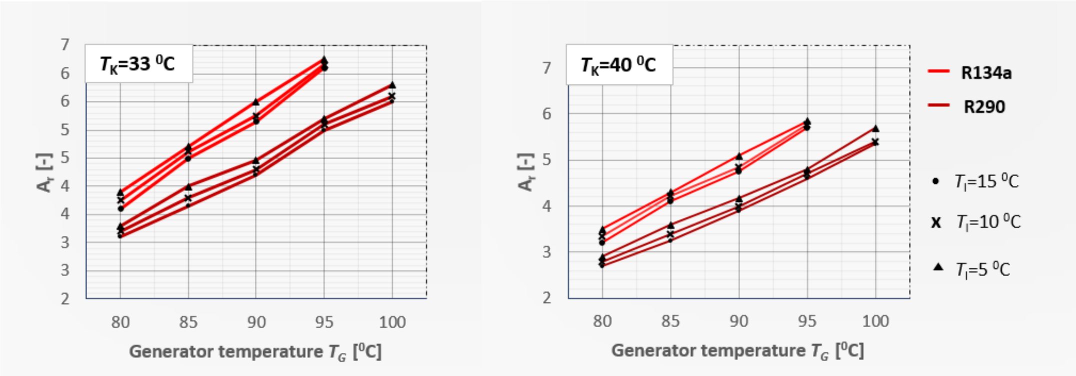

Figure 9. Effect of operating conditions on area ratio for working fluids R134a and R290.

As a nondimensional parameter, area ratio is expressed as the ratio of the cross-section areas of the mixing chamber A_3 and nozzle throat A_1 respectively. When A_r area ratio value is higher, the losses in the ejector are smaller, which causes a higher ejector entrainment ratio, and vice versa. The aforementioned interdependence of the working fluid temperature in the generator and ejector entrainment ratio means that an increase in area ratio is in direct proportion to the increase in T_G temperature (Figure 9).

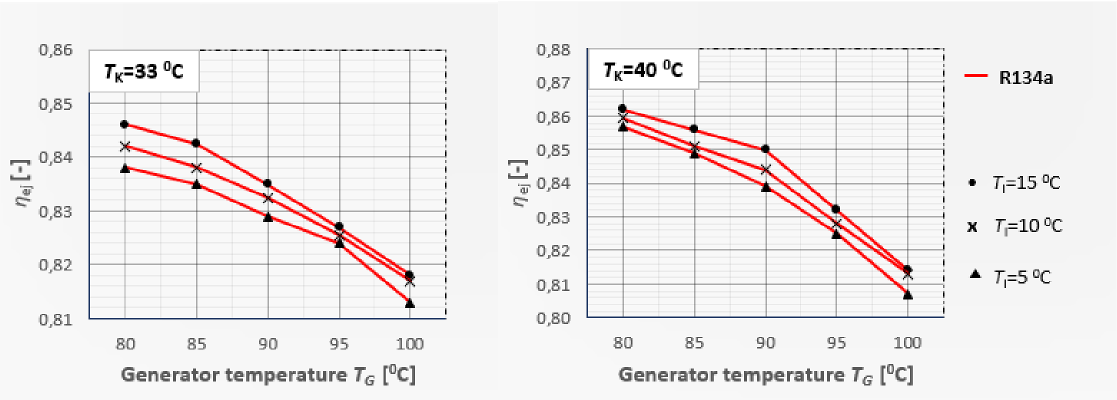

Figure 10. Effect of operating conditions on ejector efficiency for working fluid R134a.

Based on the diagram (Figure 10), it can be concluded that ejector efficiency is in inverse proportion to the working fluid temperature in the generator, which can be seen from equation (16). The equation shows that ejector efficiency decreases with the increase of generator temperature because change in the isentropic enthalpy difference during the passage through the primary nozzle is larger than that in the entertainment ratio. In a similar manner as values for COP, ejector efficiency increases with a rise in evaporation temperature. The influence of T_K temperature on ejector efficiency is insignificant, bacause of the combined effect of the increase in the enthalpy difference ($h_{K,ul}$-$h_{I,iz}$) and the decrease in ejector entrainment ratio.

The influence of nozzle and diffusor efficiencies on the COP and μ parameters for the R134a refrigerant is illustrated in Figure 11. For higher values of the nozzle and diffusor efficiencies, the throat area and the constant section rise as well, and the mass flow rate of the primary fluid from the generator decreases, which leads to an increase in the COP and μ values. Also, the nozzle and diffusor efficiency have no influence on the mass flow rate of the secondary fluid from the evaporator, and consequently, it has no influence on the cooling effect and enthalpy difference through the generator . Entrainment ratio has a higher line slope than the COP. Thus, the influence of the diffuser and noozle efficiences on entrainment is higher than that on COP. The diagram also indicates that nozzle efficiency affects the COP and μ values more than diffusor efficiency does.

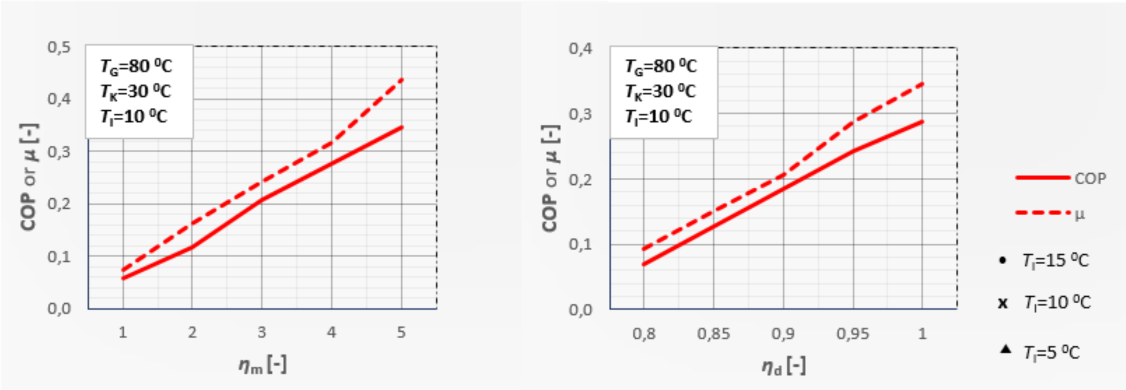

Figure 11. Effect of ejector efficiencies on system COP and entrainment ratio for working fluid R134a.

8 Conclusion

Mathematical modelling provides an efficient approach to the study of ejector performance characteristics depending on the operating conditions, geometry, refrigerant properties, etc. The presented mathematical model algorithm has been developed on the basis of a one-dimensional theoretical analysis of a low-temperature ejector cooling system and analytical equations.

Based on the fact that mixing pressure p' is lower than the pressure of the secondary fluid from the evaporator and the described thermodynamic processes and equations, a one-dimensional theoretical model of an ejector cooling system has been described in order to foresee the optimum values of μ, COP, A_r and η_{ej}. Values of ejector entrainment ratio, COP and ejector efficiency rise when the working fluid temperature in the generator rises, while the rise in working fluid temperature in the condenser leads to a gradual decrease rather than a sudden drop of these values. In addition, it can be noted that the working fluid temperature in the evaporator has a greater impact on the performance characteristics of the ejector cooling system than the working fluid temperatures in the condenser and generator.

9 References

[1] **J. M. Chen, H. Havtun, B. Palm**. Investigation of ejectors in refrigeration system: Optimum performance evaluation and ejector area ratios perspectives. Applied Thermal Engineering 2014, 64:182–191.

[2] **M. Gojak, Dj. Kozić, B. Petrović**. Thermodinamic analysis of solar-driven ejector cooling. Processing ’20, 33rd international congress on process industry.

[3] **J.L. Yu, Y.F. Ren, H. Chen, Y.Z. Li**, Applying mechanical subcooling to ejector refrigeration cycle for improving the coefficient of performance. Energy Conversion and Management 2007, 48:1193-1199.

[4] **H. El-Dessouky, H. Ettouney, I. Alatiqi, G. Al-Nuwaibit**, Evaluation of steam jet ejectors. Chemical Engineering and Processing 2002, 41:551-561.

[5] **D.W. Sun, I.W. Eames**, Performance characteristics of HCFC-123 ejector refrigeration cycles. International Journal of Energy Research 1996, 20:871-885.

[6] **B. Tashtoush, A. Alshare, S. A. Rifai**. Performance study of ejector cooling cycle at critical mode undersuperheated primary flow. Energy Conversion and Management 2015, 94:300–310.

[7] **D. Butrymowicz , K. Smierciew J. Karwacki, J. Gagan**. Experimental investigations of low-temperature driven ejection refrigeration cycle operating with isobutane 2013, International Journal of Refrigeration 39.

[8] **S. Elbel, N. Lawrence**. Review of recent developments in advanced ejector technology. International Journal of Refrigeration 2015, 62.

[9] **M. A. Redo, M. Berana, K. Saito**. Ejector refrigeration system driven by renewable energy and waste heat. 12th IEA Heat pump Conference 2017.

[10] **X. Chen, S. Omer, M.Worall, S. Riffat**. Recent developments in ejector refrigeration technologies. Renewable and Sustainable Energy Reviews 2013, 19:629-651.

[11] **R. Yapıc, H.K. Ersoy, A. Aktoprakoglu, H.S. Halkaci, O. Yigit**. Experimental determination of the optimum performance of ejector refrigeration system depending on ejector area ratio. International Journal of Refrigeration 2008, 31:1183-1189.

[12] **K. Chunnanond, S. Aphornratana.** Ejectors: applications in refrigeration technology. Renewable and Sustainable Energy Reviews 2004, 8:129-155.

[13] **R. Yapıcı, F. Akkurt**. Experimental investigation on ejector cooling system performance at low generator temperatures and a preliminary study on solar energy. Journal of Mechanical Science and Technology 2013, 26(11).

[14] **J.H. Keenan, E.P. Neumann, F. Lustwerk**. An investigation of ejector design by analysis and experiment. Journal of Applied Mechanics, Transactions ASME 1950, 72:299-309.

[15] **C. P. Arora**. Refrigeration and Air Conditioning, 3rd edition, Singapore McGraw-Hill, 2009.

[16] ***REFPROP, NIST Standard Reference Database 23, Version 8.0.